Analyst

Accepted Manuscript

ROYAL SOCIETY OF CHEMISTRY

www.rsc.org/analyst

Dual-Functional Probes for Sequential Thiols and Redox Homeostasis Sensing in Live cells

Tao Ma,[a] Hui Ding,[a] Haijiao Xu,[b] Yanlin Lv,[a] Heng Liu,[a] Hongda Wang[b*], Zhiyuan Tian[a*]

[a]School of Chemistry and Chemical Engineering, University of Chinese Academy of Sciences (UCAS), Beijing 100049, P. R. China;

[b]State Key Laboratory of Electroanalytical Chemistry, Changchun Institute of Applied Chemistry, Chinese Academy of Sciences (CAS), Changchun 130022, P. R. China

E-mail: zytian@ucas.ac.cn; hdwang@ciac.jl.cn

Abstract

A new type of resorufin-based dual-functional fluorescent probe whose fluorescence emission features are sensitive to thiol compounds and redox homeostasis was developed. Thiols-triggered nucleophilic substitution of the probes transfers the nonfluorescent probe to highly fluorescent resorufin moiety; the released resorufin not only enables fluorescence signaling specific for thiol compounds but functions as redox indicator with sensitive colorimetric and fluorescence emission change upon redox variation. The preliminary fluorescence imaging experiments have revealed the biocompatibility of the as-prepared probes and validated their practicability for thiols sensing and redox homeostasis mapping in living cells.

1 Introduction

Thiols-containing biological molecules, such as cysteine (Cys), homocysteine (Hcy) and glutathione (GSH), play crucial roles in many physiological processes, especially in maintaining the biological redox homeostasis through the equilibrium of free thiols (RSH) and disulfides (RSSR). Cysteine (Cys) deficiency is often involved in retarded growth in children, hematopoiesis decrease, leukocyte loss, skin lesions, liver damage, and weakness.[1-3] Homocysteine (Hcy) is a risk factor for cardiovascular and Alzheimer's disease, inflammatory bowel disease, neural tube effect, and osteoporosis.[4, 5] Glutathione (GSH) is the key factor for the protective and detoxifying functions of the cell in maintaining the proper thiol-disulfide status of proteins, preventing serious damage to DNA, proteins, and lipid membranes by scavenging reactive free-radical species;[5-8] and alteration of the optimum cellular thiols-disulfide zhstatus has been amalgamated with disturbance of physiological functions such as

heart disease, stroke, and other neurological disorders. Thus, it is of significant importance to develop efficient methods to detect thiols for investigating their functions in cells and disease diagnosis. It is known that a delicate redox homeostasis plays critical roles in numerous physiological functions of cells-the alterations in the redox homeostasis induced by exogenous stimuli or endogenous stress or both exerts significant influence on a host of cell functions, including but not limited to growth, differentiation, metabolism, cell cycle, stress responses, communication, migration, gene transcription, ion channels, and immune responses.[9-15] For instance, redox homeostasis acts as an important modulator in the self-renewal and differentiation of stem cells.[16-19] Additionally, redox homeostasis is a pivotal index for disease diagnosis because redox imbalance induced by oxidative stress may lead to an oncogenic stimulation, defective cell death and aberrant proliferation, and eventually contribute to the development of cancer.[20, 21] Beyond doubt, it is critical to monitor the redox state of a cell and its oscillation for an accurate evaluation of the cellular functioning and/or exploration of the relationship between the disturbances in the redox homeostasis and some diseases like cardiovascular diseases, Alzheimer's, and cancers. However, increasing evidence is now supporting the notion that informative measurement of cellular redox state might be more challenging than previously realized and the lack of effective strategy for measuring the status of intracellular redox homeostasis has been a profound limitation for basic research and practical clinical diagnosis.[22] Owing to their apparent advantages in terms of ultrahigh sensitivity, excellent spatiotemporal resolution, simplicity of manipulation and applicability to intracellular detection over other strategies, such as high performance liquid chromatography (HPLC), capillary electrophoresis (CE), electrochemical techniques, mass spectrometry, fluorescence-based approaches have played active roles at the forefront of thiols detections in recent years.[23] Most fluorescent probes for thiols developed so far are based on a salient feature of thiols, namely their strong nucleophilicity, which inherently enables high binding affinity of thiols toward specific metal ions, such as Hg^{2+}, and specific reactions between thiols and probes, such as Michael addition, cyclization reaction with aldehyde and thiols-triggered cleavage reactions. The binding of metal ions to thiols and the thiols-mediated chemical reactions of the probe result in the change in detectable fluorescence signal of the probes, which forms the basis of fluorescence-based thiols detections.[23-26] Redox-sensitive genetically encoded green fluorescent proteins (GFP) and yellow

fluorescent protein (YFP) were developed, generally by integrating a dithiol-disulfide pair into the structures of YFP and GFP, respectively, and used as probes for imaging of intracellular redox potential.[22, 27-30] Very recently, Tang and co-workers reported small-molecular-weight fluorescent probes for real-time reversible imaging of redox status changes in vivo and mapping of superoxide anion fluctuations in live cells and in vivo, respectively, which clearly demonstrates the salient features of the synthesized probes in terms of sensitivity for mapping redox homeostasis and molecular events involved in redox regulation.[31, 32]

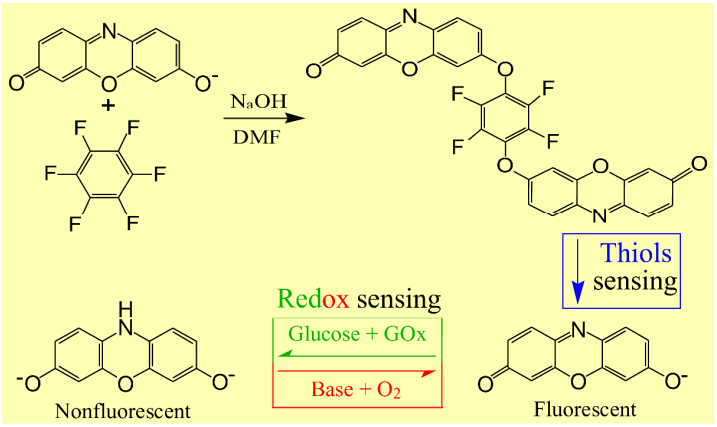

Scheme 1. Synthesis of the dual-functional probes and their sequential responses to thiols and redox homeostasis.

In the present work, a new type of dual-functional probe capable of sequential thiols detection and redox homeostasis evaluation was developed by nucleophilic substitution of hexafluorobenzene with two resorufin units at para position, as shown in Scheme 1. The as-prepared probes underwent thiol-mediated cleavage of the strong electron-withdrawing tetrafluorobenzene group, which converts nonfluorescent resorufin-based ether to fluorescent resorufin units and therefore enables thiols sensing.[23-26] It deserves mentioning that, in this work, the thiols-mediated release of resorufin not only enables fluorescence signaling specific for thiols but also generates redox indicator for redox homeostasis evaluation because the fluorescent resorufin serves as an electron acceptor and can be reduced to nonfluorescent dihydroresorufin, which can be reoxidized to resorufin.[33] It is known that, as a typical strategy, sulfonate ester and sulfonamide derivatives have been developed as probes for thiols sensing based on thiol-triggered removal of the strong electron-withdrawing 2,4-dinitrobenzenesulfonyl group from the probes and release of fluorophores such as fluorescein, naphthalimide, benzoxadiazole derivatives, and resorufin for fluorescence

signaling.[24, 34-38] Resorufin derivatives have been used as probes for enzyme activity, glucose oxidase-catalyzed oxidation of glucose, oxygen[33] and hydrogen peroxide.[39] However, the exploitation of resorufin-based dual-functional probes for sequential thiols detections and redox homeostasis evaluation has been unexplored to date. The applicability of the as-prepared probes for thiols sensing and redox homeostasis mapping in live cells was confirmed, which is the first paradigm where a single probe functions for intracellular thiols sensing and redox homeostasis mapping.

2 Experimental

2.1 Chemicals

NaHS and other metal ion inorganic salts used in the experiments were obtained from Shanghai Shenbo Chemical Co., Ltd., China. Acetonitrile (CH_3CN) and other organic reagents were purchased from Aladdin Chemistry Co., Ltd., China. Biological reagents were purchased from Acros and Aldrich. All the reagents were analytical reagent grade and used without purification. All solutions were freshly prepared before use. Milli-Q ultrapure water (18.2 MΩcm) was used in all experiments.

2.2 Apparatus

The structural information of the probe was obtained in transmission mode on a Fourier-transform infrared spectrophotometer (FT-IR, American Nicolet Corp. Model 170-SX) using the KBr pellet technique. ^{1}H NMR spectra were measured on a Brucker DMX-400 spectrometer at 400 MHz in $CDCl_3$ with tetramethylsilane as the internal standard. Fluorescence emission spectra were recorded with a Fluoromax-4 spectrofluorometer instrument.

2.3 Synthesis

To a mixture of hexafluorobenzene (37.2mg, 0.2mmol) and resorufin sodium salt (105.8mg, 0.45mmol) in DMF (10mL) in ice-water bath, NaOH (16mg, 0.4mmol) was added and the resulting mixture was stirred at room temperature for 12 h until the completion of the reaction confirmed by TLC. Water (10 mL) was subsequently added and the mixture was extracted with ethyl acetate (30 mL), washed with brine (30 mL), and dried with anhydrous magnesium sulfate and then concentrated in vacuum. After solvent removal, the crude product was purified by silica gel column chromatography to give yellow product 78mg, yield: 68%. The structure of compound was confirmed by mass spectrometry, IR spectra, and ^{1}H -NMR spectroscopy. FT-IR (KBr) ν (cm^{-1})：2961, 1726, 1600, 1514, 1284, 1123, 1076, 787. ^{1}H-NMR (300 MHz, $CDCl_3$): δ (ppm)

7.71 (d, *J*=1.2, 2H), 7.65 (d, *J*=4.8, 2H), 7.63 (s, 2H), 7.57 (s, 2H), 7.53 (d, *J*=1.5, 2H), 7.48 (d, *J*=4.8, 2H). MALDI-TOF MS: 572.1(M^+).

2.4 UV-visible absorption and fluorescence spectral study

Stock solutions of Cys, GSH and NaHS, respectively, in distilled water and the probe in acetonitrile (CH_3CN) were prepared before UV-visible absorption and fluorescence emission measurements. In a typical spectral measurement, aqueous sample of the probe was prepared by adding small aliquots of the probe/CH_3CN stock solution into a cuvette with 2 mL of 0.2 M 3-(*N*-morpholine) propanesulfonic acid (MOPS) buffer (pH 7).

2.5 General procedure for cell imaging

Macrophages were cultured in media (GIBCO RPMI 1640 supplemented with 10%FBS, 100 units/mL of penicillin and 100 units/mL of streptomycin) at 37 ℃ in a humidified incubator, and culture media were replaced with fresh media every day. The cells were treated with 1mM NEM (*N*-ethylmaleimide) in culture media for 30 min at 37℃ and then washed with phosphate buffered saline (PBS) before experiment. The cells were further incubated with 5 μM of probe in culture media for 15min at 37℃ and then washed 3 times with warm PBS buffer before cell fluorescence imaging experiments with confocal laser scanning microscopy.

3. Results and discussion

The target probe was synthesized via a facile nucleophilic substitution reaction of hexafluorobenzene with resorufin in the presence of NaOH with relatively high yield, approximately 68%. The aqueous solution of the target probe (4μM) is nearly colorless, as shown in Figure 1A. To evaluate the response of the as-prepared probe to thiol, UV-Vis absorption and fluorescence measurements of probe in 0.2 M MOPS buffer were performed in the absence and presence of thiol and its inorganic counterpart, NaSH salt (Figure 1). It was found that aqueous sample of probe displays weak absorption in the ultraviolet region. Upon addition of NaSH, significant absorption increase in the region of 475-600 nm with maximum peak at ~571 nm was clearly observed. As a result, the aqueous sample turned from nearly colorless to a vivid pink color (Figure 1A). The fluorescence emission features of the probe sample also exhibited obvious change upon addition of NaSH. Specifically, emission intensity of the sample at 583 nm dramatically augmented 13-fold upon addition of 3 equiv of NaSH and the sample presented a bright orange fluorescence color in contrast to the

weak fluorescence of the sample prior to addition of NaHS (Figure 1B).

To evaluate the ability of the as-prepared probe for biothiols sensing, the fluorescence emission features of the probe were investigated in the presence of cysteine (Cys) with the result illustrated in Figure 1C. It can be seen that the emission intensity at 583 nm gradually increased with increasing the amount of Cys. Figure 1D displays a plot of $(I-I_0)/I_0$ against the concentration of Cys ranging from 0 to 50 μM and the corresponding linear fit (R^2 = 0.998) to the experimental data. I_0 is the emission intensity at 583-nm of the probe in the absence of Cys and I is the counterpart intensity in the presence of different concentrations of Cys. From titrations, a detection limit of ~0.52 μM of the as-prepared probe for Cys sensing was determined based on the 3-sigma method, suggesting the possibility of quantitative detection of biothiols using the as-prepared probe.

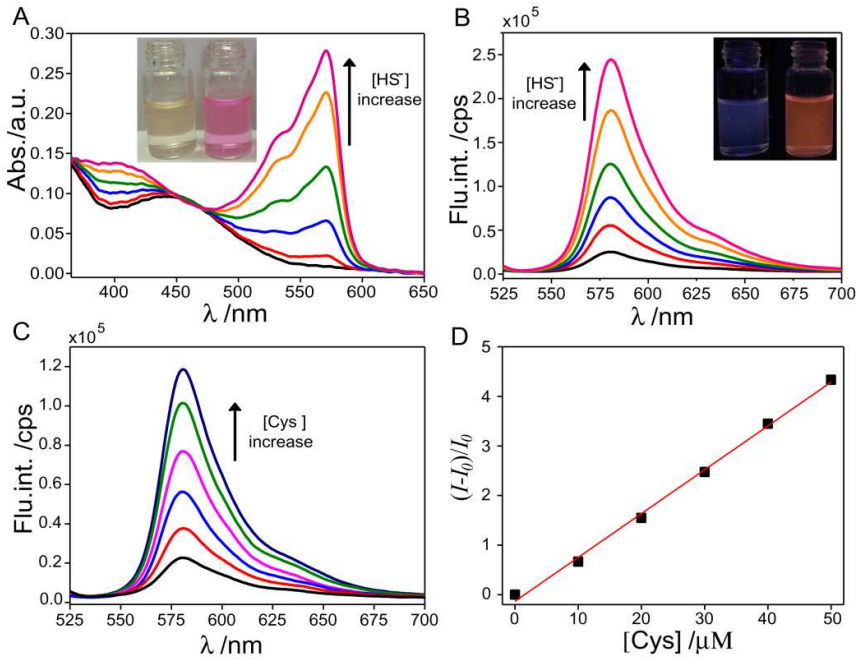

Figure 1. (A, B) Evolution of UV-Vis absorption and emission spectra of probe in the CH_3CN-H_2O mixed solvent upon the addition of NaHS. Insert: photographs of aqueous sample of probe before (left) and after (right) addition of NaHS under room light (A) and 365-nm light (B) illumination. (C) Evolution of emission spectra of probe in the CH_3CN- H_2O mixed solvent upon the addition of Cys. (D) A plot of the ratio of I-I_0 over I_0 as a function of Cys concentration. The red line is a linear fit to the data (R^2=0.998). [probe] = 4μM. λ_{ex}= 510nm.

Aqueous solution of resorufin sodium salt displays intense absorption band in the region of 475-600 nm and therefore presents a vivid pink color. It is noted that the resorufin anion possesses typical intramolecular push-pull character and therefore

electron delocalization over the molecular skeleton that responsible for the intense absorption in the visible region. Owing to the strong electron-withdrawing property of tetrafluorobenzene (TFB) moiety, derivatization the 7-OH of resorufin with TFB is expected to sequestrate the negative charge of phenolate anion ($Ph\text{-}O^-$) and consequently weakens the push-pull character.[24, 34-38] As a result, the electron delocalization of resorufin moiety decreases and the weak absorption and fluorescence features in the visible region of the probe were observed. The addition of thiols and HS^- triggers the nucleophilic aromatic substitution reaction of the probe and eventually leads to cleavage of the ether bond of probe and the release of resorufin moiety. Consequently, push-pull character of resorufin moiety was recovered and the retrieved intense absorption features in the visible region and clear fluorescence enhancement were observed.

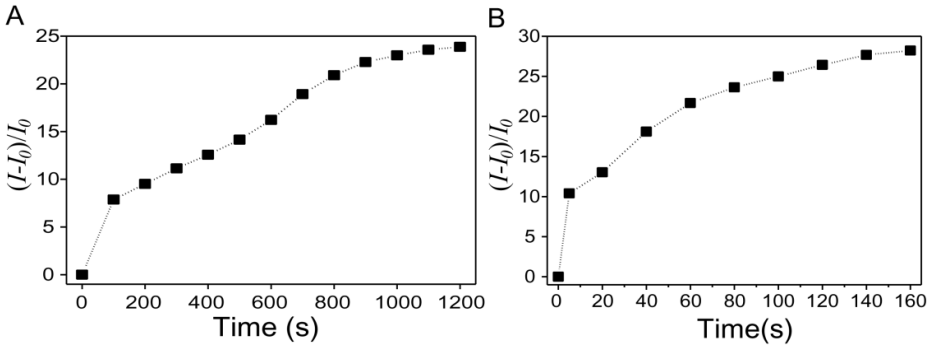

Figure 2. Evolution of the emission intensity (at 583-nm) of the probe (10μM) in the presence of 100 equiv. of Cys (A) and NaHS (B) in 0.2 M MOPS buffer of pH 7.0.

As demonstrated in Figure 1, both Cys and HS^- were capable of retrieving the fluorescence of resorufin moiety by triggering the cleavage of the ether bond of probe. However, the fluorescence emission features of the probe exhibited distinct dynamic changes upon addition of Cys and HS^-, respectively. As shown in Figure 2A, fluorescence intensity of the probe exhibited a ~10-fold enhancement 200 s after the addition of excess amount of Cys and approached a maximum of ~24-fold increase after 20 min. In sharp contrast, fluorescence intensity of the probe exhibited an enhancement of more than 10-fold in 5 s after addition of excess amount of HS^- and reached a plateau after 160 s with 28-fold fluorescence enhancement. Such discrepancy in the response of the probe to HS^- and Cys suggested the difference in reaction rate of the probe with different thiol compounds. Specifically, the release of fluorescent resorufin moiety from the probe is based on thiol-mediated rupture of the C (TFB)-O bond and nucleophilic aromatic substitution reaction of probe, in which

the Cys component was expected to suffer from stronger steric hindrance effect owing to its large size as compared to that of HS^-.

To evaluate the sensing selectivity of the as-prepared probes for Cys, the probes were tested against various other typical essential amino acids such as Ser, Gly, Leu, Glu, Arg, Lys, Ala, Pro, Phe, and Tyr as well as the thiol-containing GSH. The response time of the probe to Cys and various other amino acids were 5 min. As illustrated in Figure 3, upon addition of these reference amino acids or GSH with identical concentrations, the fluorescence emission intensities of the probes nearly kept unchanged in the cases of reference amino acids or minimally affected in the case of GSH as compared to the original probe sample. In sharp contrast, the addition of Cys with identical concentrations induced ~5-fold fluorescence enhancement. These results suggest a high selectivity of the as-prepared probes for thiols over other amino acids and indicate the diagnostic potential of the probes for thiols sensing in biological samples.

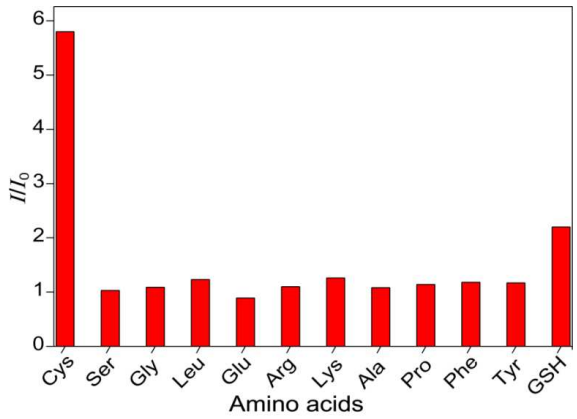

Figure 3. Fluorescence response of probe (10 μM) to typical essential amino acids and GSH (10 μM). I_0 and I represent the fluorescence intensity (at 583-nm) of the probe in the absence and presence of the corresponding amino acids or GSH.

Owing to its superior characteristics such as high extinction coefficient, high fluorescence quantum yield, good water-solubility, good photostability, and biocompatibility, resorufin has been used greatly for different detection schemes such as proteases[40, 41], ions[42, 43] and reactive oxygen species (ROS)[44, 45]. Another salient feature of resorufin is its redox activity, namely it potential acting as a redox indicators [46]. Specifically, the fluorescent resorufin can be reversibly reduced to another colorless and nonfluorescent derivative of resorufin, dihydroresorufin, and the latter can be reoxidized to resorufin by dissolved oxygen in alkaline aqueous milieu.

Owing to its redox activity, resorufin has been used in anaerobic microbiology to indicate contamination with oxygen[47], in glucose oxidase-catalyzed oxidation of glucose as electron acceptor[48], and in tracing dissolved oxygen[33]. Thus, thiol-triggered cleavage of the ether bond of the probe in the present work not only imparted fluorescence signaling for thiols sensing but also released active redox indicators for subsequent redox mapping in a reversible manner.

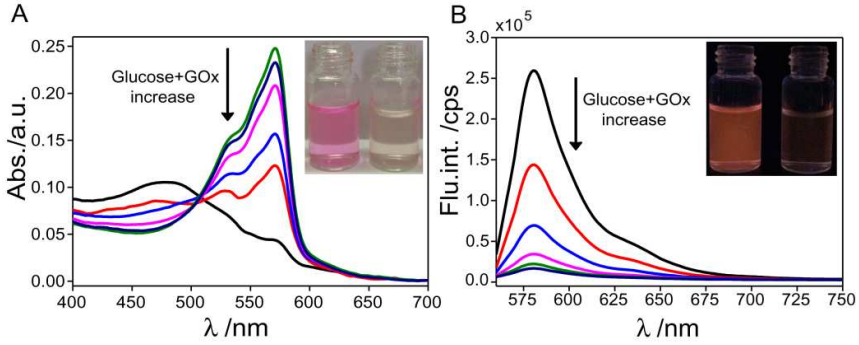

Figure 4. Evolution of UV-Vis absorption (A) and fluorescence emission spectra (B) of probe in the CH_3CN- H_2O mixed solvent after NaHS treatment upon the addition of glucose and glucose oxidase (GOx). [probe] = 4μM. λ_{ex}= 550 nm. Insert: photographs of aqueous sample of probe before (left) and after (right) treatment of glucose and GOx under room light (A) and 365-nm light (B) illumination.

To evaluate the redox sensing ability of the probe, small aliquots of aqueous GOx and glucose solution were added to the aqueous sample of the probe (4μM) after thiols treatment and the UV-Vis absorption and fluorescence emission spectra of the sample were then recorded. As shown in Figure 4A, the characteristic absorption with maximum peak at ~571 nm gradually decreased upon increasing amount of glucose and GOx added to the sample and the vivid pink color of the sample gradually faded and regressed to colorless. Accompanying the obvious change in absorption features, fluorescence emission of the probe sample underwent remarkable regression upon addition of glucose and GOx, as shown in Figure 4B. Specifically, only ~5% of the initial emission intensity of the aqueous probe sample remained after incubation with 25 equiv. of glucose and fluorescence of the sample became extremely faint from bright orange color before reduction treatment. Such remarkable changes in absorption and fluorescence emission features upon reduction treatment originate from the difference in the electronic configuration between the resorufin and dihydroresorufin. Specifically, reduction treatment on resorufin essentially deprived resorufin of it push-pull character and led to the formation of dihydroresorufin with limited electron delocalization features. As a result, significantly decreased absorption

and fluorescence features in the visible region of the probe were observed.

Figure 5 displays the absorption and fluorescence emission features of the aqueous probe sample after sequential thiols and reduction treatment upon following addition of aqueous NaOH solution under aerobic conditions. It was found that the colorless solution immediately changed to pink upon addition of small amount of NaOH under aerobic conditions and a solution with nearly completely restored vivid pink color was obtained when 2 equiv. of NaOH was added to the sample. As shown in Figure 5A, upon increasing amount of NaOH added to the probe sample, the characteristic absorption band centered at ~571 nm gradually increased and meanwhile the fluorescence emission of the probe sample centered at ~583 nm significantly augmented. Specifically, addition of 2 equiv. of NaOH to the sample led to ~16-fold fluorescence enhancement and the aqueous sample eventually restored to the bright orange fluorescence color from the faint fluorescence before re-oxidization treatment. Contrary to the reduction treatment, oxidization of dihydroresorufin by dissolved oxygen in alkaline milieu led to the recovery of resorufin and essentially restored the push-pull character of the probe.

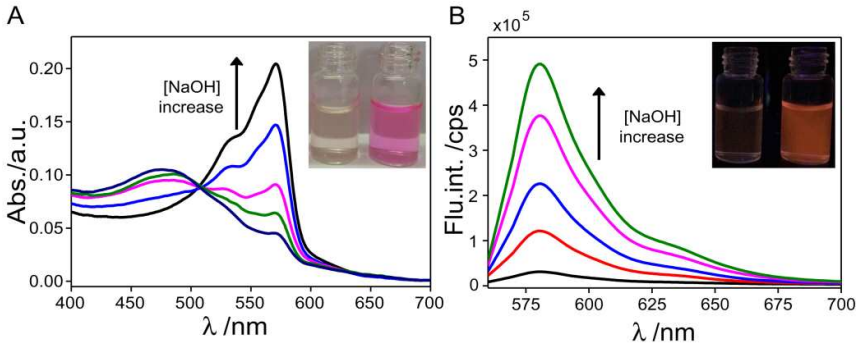

Figure 5. Evolution of UV-Vis absorption (A) and fluorescence spectra (B) of probe in the CH_3CN-H_2O mixed solvent after NaHS and reduction treatment upon the addition of NaOH under aerobic conditions. λ_{ex}= 550 nm. Insert: photographs of aqueous sample of probe before (left) and after (right) addition of NaOH under room light (A) and 365-nm light (B) illumination.

As illustrated in Figure 1 and Figure 4, the probe sample underwent marked augment in fluorescence emission upon addition of thiol species and the following addition of redox species, i.e. GOx and glucose aqueous solution, conversely led to remarkable decrease in fluorescence emission. For a real target sample with the co-existence of thiol components and redox species, it is generally a concern whether the existence of one component perturbs the sensing of another. Figure 6 A displays the emission features of the probe prior to and after the addition of NaHS. It can be

seen that the fluorescence intensity of the probe exhibited an ~11-fold enhancement upon the addition of excess amount of NaHS. Figure 6 B displays the emission features of the probe sample in the absence of thiol components and redox species and of the sample in the co-existence of thiol components and redox species. It can be seen that the fluorescence emission of the sample immediately displayed a ~7-fold enhancement in the emission intensity at 583-nm as compared to the emission spectrum of the sample before the addition of thiol components and redox species (line 2). Upon the following 10-minute storage of the sample at 37□, fluorescence emission of the sample with remarkable regression was clearly observed (line 3). This means that the probe sample is capable of sensing thiol components and redox species in a sequential way even in the co-existence of them. Moreover, fluorescence emission of the probe sample significantly augmented upon the following addition of NaOH solution under aerobic conditions (line4), consistent with the change observed from the aforementioned sequential sensing study results.

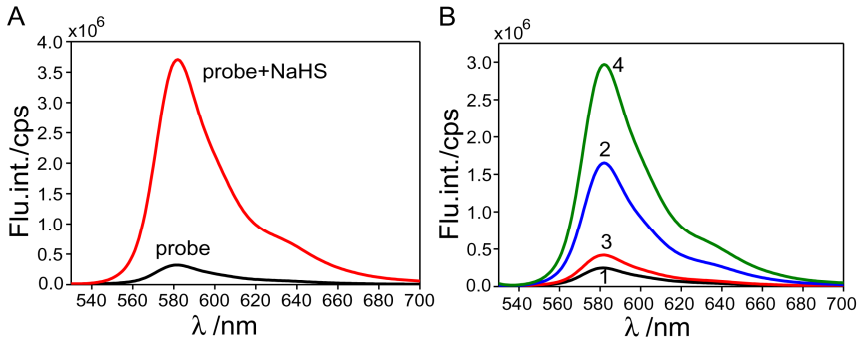

Figure 6. (A) Fluorescence emission spectra of probe sample prior to and after the addition of NaHS. (B) Fluorescence emission spectrum of the probe sample in the absence of NaHS, glucose, GOx and NaOH (line 1), that of the sample acquired immediately after the simultaneous addition of NaHS, glucose and GOx (line 2), that of the sample acquired after 10-minute storage at 37□ following the acquisition of line 2 (line 3), and that of the sample for acquisition of line 3 with the following addition of aqueous NaOH solution under aerobic conditions (line 4).

Figure 7 displays the recoverability of fluorescence emission of the probe after thiols treatment upon alternating reduction and re-oxidization. It can be seen that the fluorescence intensity decreased significantly upon addition of glucose and GOx. Upon the subsequent addition of aqueous NaOH solution under aerobic conditions, such reduction-induced fluorescence decrease could be completely offset and the fluorescence intensity reverted to the level prior to the addition of glucose and GOx. The following reduction/oxidization cycle under sequential addition of glucose and

GOx and NaOH also demonstrated recoverability of the fluorescence emission features of the probe. For several cycles, at least, such reduction-induced fluorescence decrease and then oxidization-induced fluorescence restoration were fully reversible, as shown in Figure 7, suggesting the excellent photostability and the potential of such probes for multiple-cycle redox mapping applications.

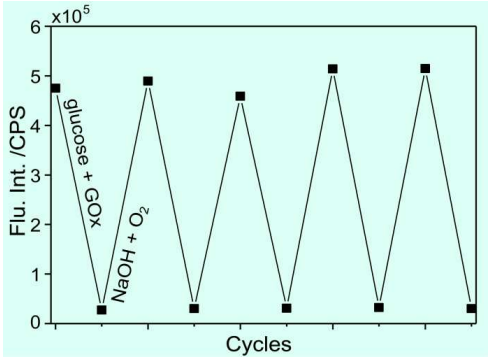

Figure 7. Fluorescence change of the aqueous probe sample after thiols treatment upon cyclic reduction-oxidation treatment.

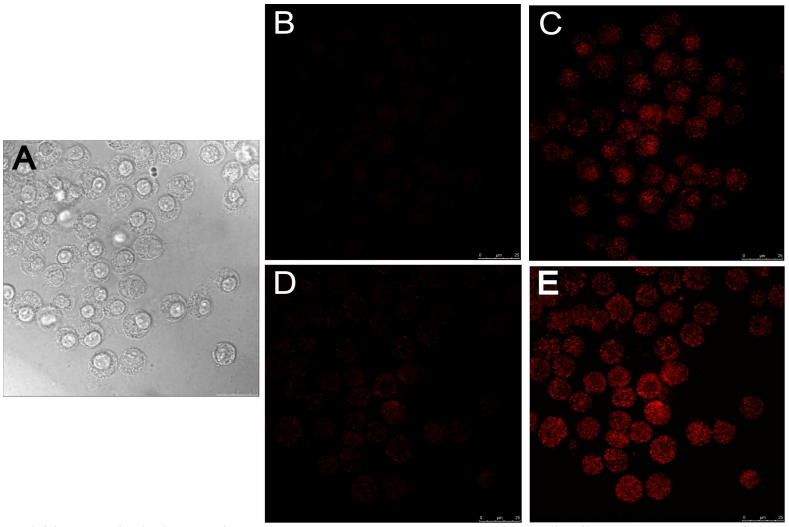

Figure 8. Differential interference contrast (DIC) and fluorescence images of the probe in intracellular thiols and redox sensing. (A and B) The DIC and fluorescence images of cells after sequential incubations with NEM and the probe; (C) the fluorescence image of cells shown in (B) after following incubation with NaHS; (D) the fluorescence image of cells shown in (C) after following incubation with reductant (glucose and GOx); (E) the fluorescence image of cells shown in (D) after following incubation with NaOH under aerobic conditions. λ_{ex}= 561 nm.

The applicability of the as-prepared probes for thiols sensing and redox homeostasis evaluation in live cells was also confirmed. The Macrophages cell lines were used as the model because of their ability to efficiently endocytose cellular

debris, pathogens, exogenous particles and molecules. To exclude the influence of interfering cellular fluorescence originating from the reaction of endogenous thiol compounds including Cys and GSH in cells with the probe, the cells were pretreated by thiolblocking reagent *N*-ethyl maleimide (NEM), a trapping reagent of thiol species prior to the incubation of cells with probe.[24] Specifically, the Macrophages cells were incubated with NEM (1mM) for 30 min and then incubated with probe (20 μM) for 15 min before the acquisition of DIC and fluorescence images of the cells (Figure 8A and B). Then Macrophages were pretreated with NaHS (20 μM) for 15 min and then the fluorescence images of the cells were acquired with confocal laser scanning microscopy (Figure 8C). It can be clearly seen that the cells with internalized probes in the absence of thiols exhibited negligible background fluorescence. In sharp contrast, the cells after incubation with NaHS exhibited strong fluorescence that clearly brightened their cellular contours (Figure 8C). Such dramatic fluorescence brightness disparity between Figure 8 B and C clearly demonstrated the usefulness of the as-prepared probe for intracellular thiols sensing. To evaluate the intracellular redox sensing ability of the probe, the cells after NaHS treatment were subsequently incubated with glucose (200 μM) and GOx (80 μg/mL) for 10 min and then the fluorescence images of the cells were acquired. As shown in Figure 8D, markedly decreased fluorescence brightness of the cells after reduction treatment was observed, in consistent to the in vitro experiment results illustrated in Figure 4. It is noted that as compared to the cells shown in Figure 8B, a little bit of cells shown in Figure 8C exhibited faint fluorescence and their cellular contours were dimly visible. Such faint fluorescence might be attributable to those residual resorufin moieties that did not react with the reductant in cells. Following the reduction treatment and image acquisition, 1μL of aqueous NaOH solution (10 mM) was added to the medium in cell culture dish with inlet oxygen and the incubation was kept for 10 min before fluorescence image acquisition. As illustrated in Figure 8E, fluorescence brightness of the cells after the treatment of NaOH under aerobic conditions was completely restored to the level prior to the reduction treatment (Figure 8C). Beyond doubt, such excellent fluorescence recoverability of the probe in intracellular milieu upon the redox reaction cycle suggests the usefulness of the as-prepared probes for cell redox homeostasis mapping.

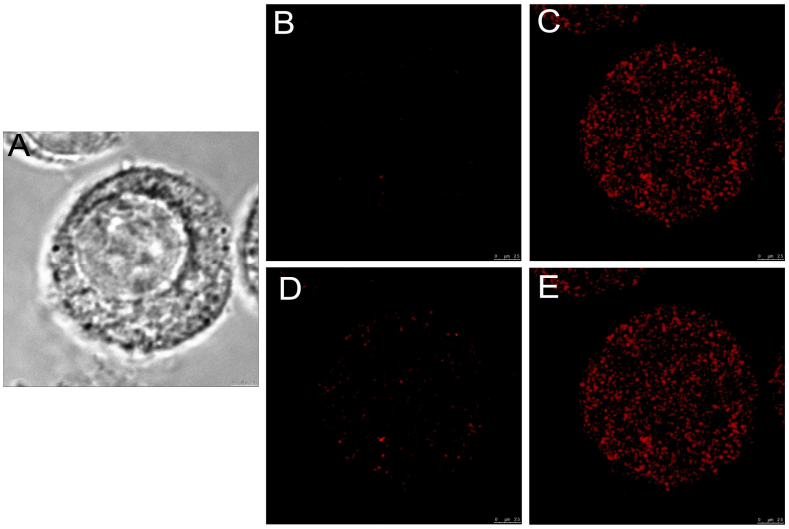

Figure 9. DIC and confocal fluorescence images of Macrophage monoplast with internalized probes. (A and B) DIC and fluorescence images of a monoplast after sequential incubations with NEM and the probe; (C) the fluorescence image of the cell shown in (B) after following incubation with NaHS; (D) the fluorescence image of the cell shown in (C) after following incubation with reductant (glucose and GOx); (E) the fluorescence image of the cell shown in (D) after following incubation with NaOH under aerobic conditions. λ_{ex}= 561 nm.

Figure 9 displays the high magnification DIC and confocal fluorescence images of a Macrophage monoplast that had been pretreated with NEM, subsequently incubated with probes for thiols sensing and redox homeostasis mapping. The fluorescence images acquired after NaHS treatment (Figure 9C) and oxidization (Figure 9E) clearly indicate internalization of the probes by the Macrophage. It can be seen that the spotted fluorescence light up the cytoplasm, cell organelles, and the nuclear membrane area, indicating a good appetite of the cell for the probes. Additionally, these images definitely demonstrate the sequential thiols sensing and redox homeostasis mapping abilities of the probes in cells, which is consistent with the cell imaging results shown in Figure 8. It also deserves mentioning that the probes did not appear to exhibit appreciable cytotoxicity under the incubation time and loading concentration in the cell imaging experiments in the present work.

4. Conclusion

To conclude, we have developed a new type of dual-functional fluorescent probe whose fluorescence emission features are sensitive to thiol compounds and redox homeostasis. Specifically, thiol compounds may induce the transfer of the

resorufin-based nonfluorescent probe to highly fluorescent resorufin moiety; the released resorufin not only enables fluorescence signaling specific for thiol compounds but functions as redox indicator with sensitive colorimetric and fluorescence emission change upon redox variation. A detection limit of 0.52 μM of the as-prepared probes for Cys was determined and the preliminary fluorescence imaging experiments have revealed the biocompatibility of the as-prepared probes and validated their practicability for thiols sensing and redox homeostasis mapping in living cells. This is first paradigm where a single probe functions for intracellular thiols sensing and redox homeostasis mapping and is therefore potentially useful in bioresearch and disease diagnosis in the future.

Acknowledgements

T. Ma, H. Ding and H. J. Xu contributed equally to this work. Financial support from the National Natural Science Foundation of China (grant no. 21173262 and 21373218) and the "Hundred-Talent Program" of CAS to ZT are acknowledged.

References

1. B. Han, J. Yuan and E. Wang, *Anal. Chem.*, 2009, 81, 5569-5573.
2. S. Shahrokhian, *Anal. Chem.*, 2001, 73, 5972-5978.
3. Y. Zhang, Y. Li and X.-P. Yan, *Anal. Chem.*, 2009, 81, 5001-5007.
4. M. Refsum, H., M. Ueland, P. M., M. Nygård, O. and M. Vollset, Dr.PH, S. E., *Annu. Rev. Med.*, 1998, 49, 31-62.
5. S. Seshadri, A. Beiser, J. Selhub, P. F. Jacques, I. H. Rosenberg, R. B. D'Agostino, P. W. F. Wilson and P. A. Wolf, *N. Engl. J. Med.*, 2002, 346, 476-483.
6. Y. Gao, Y. Li, X. Zou, H. Huang and X. Su, *Anal. Chim. Acta*, 2012, 731, 68-74.
7. R. Hong, G. Han, J. M. Fernández, B.-j. Kim, N. S. Forbes and V. M. Rotello, *J. Am. Chem. Soc.,* 2006, 128, 1078-1079.
8. Z. A. Wood, E. Schröder, J. Robin Harris and L. B. Poole, *Trends Biochem. Sci.*, 2003, 28, 32-40.
9. H. Jay Forman and M. Torres, *Mol. Asp. Med*, 2001, 22, 189-216.
10. H. J. Forman and M. Torres, *Am. J. Respir. Crit. Care. Med.*, 2002, 166, S4-S8.
11. Y. Liu and D. D. Gutterman, *Clin. Exp. Pharmacol. Physiol.*, 2002, 29, 305-311.
12. W. Dröge, *Free Radicals in the Physiological Control of Cell Function*, 2002.
13. M. Rojkind, J. A. Domínguez-Rosales, N. Nieto and P. Greenwel, *CMLS, Cell. Mol. Life Sci.*, 2002, 59, 1872-1891.
14. C. H. Foyer and G. Noctor, *The Plant Cell Online*, 2005, 17, 1866-1875.

15. B. Morgan, D. Ezeriņa, T. N. E. Amoako, J. Riemer, M. Seedorf and T. P. Dick, *Nat Chem Biol*, 2013, 9, 119-125.
16. C. Chen, Y. Liu, R. Liu, T. Ikenoue, K.-L. Guan, Y. Liu and P. Zheng, *J. Exp. Med.*, 2008, 205, 2397-2408.
17. M. M. Juntilla, V. D. Patil, M. Calamito, R. P. Joshi, M. J. Birnbaum and G. A. Koretzky, *AKT1 and AKT2 maintain hematopoietic stem cell function by regulating reactive oxygen species*, 2010.
18. S. Chuikov, B. P. Levi, M. L. Smith and S. J. Morrison, *Nat Cell Biol*, 2010, 12, 999-1006.
19. K. Wang, T. Zhang, Q. Dong, E. C. Nice, C. Huang and Y. Wei, *Cell Death Dis*, 2013, 4, e537.
20. M. J. Percy, P. W. Furlow, G. S. Lucas, X. Li, T. R. J. Lappin, M. F. McMullin and F. S. Lee, *N. Engl. J. Med.*, 2008, 358, 162-168.
21. Y. Mizutani, H. Nakanishi, K. Yamamoto, Y. N. Li, H. Matsubara, K. Mikami, K. Okihara, A. Kawauchi, B. Bonavida and T. Miki, *J. Clin. Oncol.*, 2005, 23, 448-454.
22. M. Gutscher, A.-L. Pauleau, L. Marty, T. Brach, G. H. Wabnitz, Y. Samstag, A. J. Meyer and T. P. Dick, *Nat Meth*, 2008, 5, 553-559.
23. X. Chen, Y. Zhou, X. Peng and J. Yoon, *Chem. Soc. Rev.*., 2010, 39, 2120-2135.
24. K. Cui, Z. Chen, Z. Wang, G. Zhang and D. Zhang, *Analyst*, 2011, 136, 191-195.
25. Z. Guo, S. Nam, S. Park and J. Yoon, *Chem. Sci.*, 2012, 3, 2760-2765.
26. Q.-Q. Wu, Z.-F. Xiao, X.-J. Du and Q.-H. Song, *Chem. Asian J.*, 2013, 8, 2564-2568.
27. H. Østergaard, A. Henriksen, F. G. Hansen and J. R. Winther, *Shedding light on disulfide bond formation: engineering a redox switch in green fluorescent protein*, 2001.
28. G. T. Hanson, R. Aggeler, D. Oglesbee, M. Cannon, R. A. Capaldi, R. Y. Tsien and S. J. Remington, *J. Biol. Chem.*, 2004, 279, 13044-13053.
29. C. T. Dooley, T. M. Dore, G. T. Hanson, W. C. Jackson, S. J. Remington and R. Y. Tsien, *J. Biol. Chem.*, 2004, 279, 22284-22293.
30. V. V. Belousov, A. F. Fradkov, K. A. Lukyanov, D. B. Staroverov, K. S. Shakhbazov, A. V. Terskikh and S. Lukyanov, *Nat Meth*, 2006, 3, 281-286.
31. W. Zhang, P. Li, F. Yang, X. Hu, C. Sun, W. Zhang, D. Chen and B. Tang, *J. Am. Chem. Soc.*, 2013, 135, 14956-14959.
32. K. Xu, M. Qiang, W. Gao, R. Su, N. Li, Y. Gao, Y. Xie, F. Kong and B. Tang, *Chem. Sci.*, 2013, 4, 1079-1086.
33. H. Golnabi and M. Razani, *Sens. Actuators B*, 2007, 122, 109-117.
34. H. Maeda, H. Matsuno, M. Ushida, K. Katayama, K. Saeki and N. Itoh, *Angew. Chem. Int. Ed.* 2005, 44, 2922-2925.
35. W. Jiang, Q. Fu, H. Fan, J. Ho and W. Wang, *Angew. Chem. Int. Ed*., 2007, 46, 8445-8448.
36. J. Bouffard, Y. Kim, T. M. Swager, R. Weissleder and S. A. Hilderbrand, *Org.*

Lett., 2007, 10, 37-40.
37. W. Zhang, R. Zhang, J. Zhang, Z. Ye, D. Jin and J. Yuan, *Anal. Chim. Acta*, 2012, 740, 80-87.
38. R. Jain and L. A. Cohen, *Tetrahedron*, 1996, 52, 5363-5370.
39. Y. Hitomi, T. Takeyasu, T. Funabiki and M. Kodera, *Anal. Chem.*, 2011, 83, 9213-9216.
40. Z. Li, X. Li, X. Gao, Y. Zhang, W. Shi and H. Ma, *Anal. Chem.*, 2013, 85, 3926-3932.
41. L. D. Lavis, T.-Y. Chao and R. T. Raines, *Chem. Sci.*, 2011, 2, 521-530.
42. M. G. Choi, J. Hwang, S. Eor and S.-K. Chang, *Org. Lett.*, 2010, 12, 5624-5627.
43. X. Ma, J. Wang, Q. Shan, Z. Tan, G. Wei, D. Wei and Y. Du, *Org. Lett.*, 2012, 14, 820-823.
44. E. W. Miller, O. Tulyathan, E. Y. Isacoff and C. J. Chang, *Nat Chem Biol*, 2007, 3, 263-267.
45. Y. Zhang, W. Shi, X. Li and H. Ma, *Sci. Rep.*, 2013, 3.
46. P. Tratnyek, T. Reilkoff, A. Lemon, M. Scherer, B. Balko, L. Feik and B. Henegar, *Chem. Educ.*, 2001, 6, 172-179.
47. P. A. Rublee, *AM BIOL TEACH*, 1984, 46, 63.
48. H. Maeda, S. Matsu-Ura, T. Senba, S. Yamasaki, H. Takai, Y. Yamauchi and H. Ohmori, *Chem. Pharm. Bull.*, 2000, 48, 897-902.

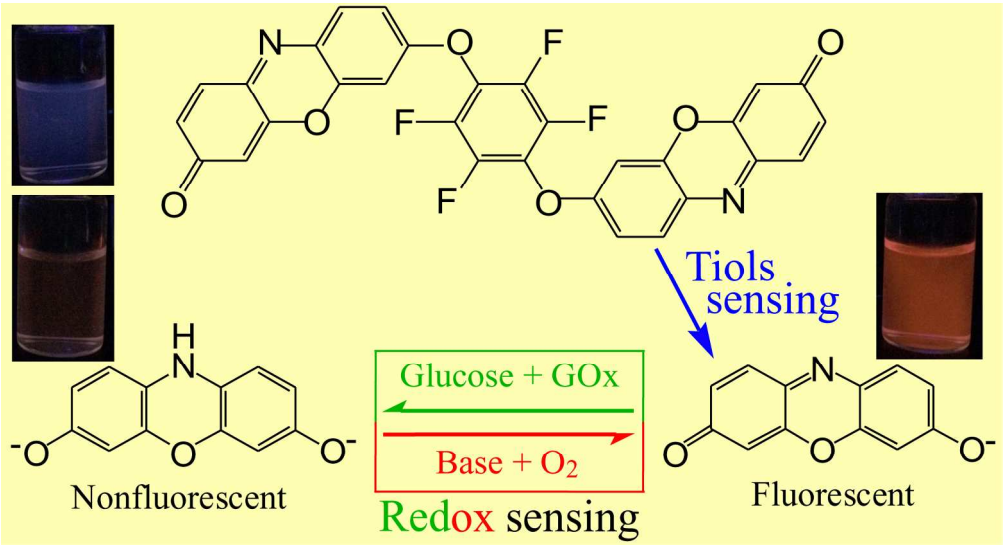

181x97mm (300 x 300 DPI)